

# MOLECULAR AND CELLULAR MAPPING OF THE VOLTAGE-DEPENDENT $\text{Na}^+$ CHANNEL

KIMON J. ANGELIDES AND THOMAS J. NUTTER

*Departments of Biochemistry and Molecular Biology and Neuroscience, University of Florida College of Medicine, Gainesville, Florida 32610*

Propagation of the action potential in nerve and muscle is a result of rapid and precisely controlled voltage-dependent changes in the membrane permeability to  $\text{Na}^+$  and  $\text{K}^+$ . The selective permeability of  $\text{Na}^+$  is modulated by the action of the  $\text{Na}^+$  channel, which forms an actual pore that traverses the membrane and is regulated by a transmembrane voltage to a sequence of resting, open, and closed states during excitation.

A number of neurotoxins are specific for this channel and have been used as molecular probes of the structure, function, and development of the channel (for a review see reference 1). Toxins that are specific for the channel include tetrodotoxin (TTX), which blocks  $\text{Na}^+$  conductance; batrachotoxin (BTX), which stabilizes a permanently open form of the channel; scorpion toxins, such as toxin V from *Leiurus quinquestriatus* (Lqq V), that specifically slow down the inactivation of the channel; and the scorpion toxins, such as toxin II from *Centruroides suffusus* (Css II), that induce repetitive firing due to the apparition of abnormal activation kinetics.

We have examined the molecular arrangement of the important functional sites on the  $\text{Na}^+$  channel by using biologically active fluorescent and photoactivatable-fluorescent derivatives of TTX (2), BTX (Angelides, K. J. and G. B. Brown, submitted for publication), Lqq V<sup>1</sup> (2a), and Css II<sup>2</sup> (2b) to determine the location of the receptor sites of the channel, to describe the conformational transitions and microenvironments of the receptor sites (2,2a–2c) and to visualize  $\text{Na}^+$  channel distribution in excitable cells microscopically. We report here on the arrangement and intramembrane location of the molecular components of the  $\text{Na}^+$  channel as determined by fluorescence resonance energy transfer, and propose a three-dimensional model of the molecular structure of the  $\text{Na}^+$  channel in excitable membranes. Portions of this work have appeared in abstract form (3).

## METHODS

Steady-state efficiencies of energy transfer were measured by both quenching of donor fluorescence and sensitized emission of the acceptor. To evaluate distances between multiple donor-acceptor pairs, the posi-

tions of the chromophores were exchanged. Limits on the range of calculated distances between the sites were evaluated by using several donor-acceptor pairs, from the fluorescence anisotropy of the energy donor, the energy acceptor, and from the depolarization of the transferred excitation (4). The distance range is further narrowed because these probes show depolarization from a combination of mixed polarization and local rotation.

The intramembrane position of the Lqq V-binding site was measured from the fluorescence quenching of DACA-Lqq V as a function of the membrane surface acceptor density and analyzed with a parallel infinite planes model (5). The acceptor was NBD-*N*-methyl-D-glucosyl-phosphatidylglycerol, which bears a carbohydrate moiety to prohibit flip-flop motion across the bilayer.

## RESULTS

The results of a series of energy transfer experiments are summarized in Table I. The binding (1), spectroscopic (2), and energy transfer distance measurements (2a–2c and Angelides and Brown, submitted for publication) indicate that the Lqq, Css, and BTX sites are sensitive to either voltage- or neurotoxin-dependent conformational changes. For example, when BTX is added to bound DACA-Lqq V, a 10-nm change to the red in the emission spectrum is seen, together with a large fluorescence enhancement. Similar effects are noted on the spectral properties of BTX-NMA, in which addition of Lqq V shifts the emission maximum ~30 nm to the red, into an environment of greater polarity, and enhances the emission intensity 10-fold. Although binding measurements indicate allosteric interactions among channel receptor sites (1), the first direct indication of molecular conformational coupling between these receptors is shown in Table I; an alteration in the receptor site distance occurs between the TTX and Lqq V receptors in the presence of BTX. In the presence of BTX, the TTX-to-Lqq distance increases to 42 Å, indicating a neurotoxin-induced conformational change in one subunit of the channel or a change in the interaction between two subunits coupled to the BTX binding site. Despite the sensitivity of the fluorescence to ligand binding, the energy transfer measurements summarized in Table I indicate that the BTX and Lqq sites are quite far apart. Thus the binding of BTX must involve conformational changes that

TABLE I  
REPRESENTATIVE ENERGY TRANSFER PARTNERS AND PARAMETERS FOR THE VOLTAGE-DEPENDENT  
SODIUM CHANNEL

Donor					Acceptor					Distance				
Name*	Channel site	$\phi$ Bound‡	$\lambda_{em}^{max}$	$r_b$	Name	Channel site	$\phi$ Bound	$\lambda_{em}^{max}$	$r_b$	E§	E	(2/3) R <sub>0</sub> Å	(2/3) R Å¶	⟨R⟩
ANT-TTX	ion-selection	0.56	398	0.18	DACA-Lqq	inactivation gate	0.33	462	0.074	0.63	0.66	34.8	32	30–35
					+ BTX-B		0.33	472	0.05		0.25	34.8	42	39–45
					NBD-Lqq	inactivation gate	0.42	526	0.137	0.45	0.48	34.3	35	32–38
NBPM-SH-Lqq	inactivation gate	0.83	366	0.121	+ BTX-B		0.42	534	0.097		0.24	34.3	42	39–45
					NMAG-TTX	ion-selection	0.67	439	0.247		0.08	18.6	32	29–36
											0.05	18.6	36	34–39
ANT-TTX	ion-selection	0.56	398	0.18	DACA-CssII	activation gate	0.72	463	0.068	0.52	0.57	34.8	33	31–36
BTX-NMA	activation & inactivation gate	0.67	408 435**	0.032 0.062	DACA-Lqq	inactivation gate	0.33	472	0.05	0.35	0.32	33.8	38	35–40
DACA-Css	activation gate	0.72	453	0.068	NBD-LqqV	inactivation gate	0.42	526	0.137	0.93	0.96	36.2	22	20–24
DACA-Lqq	inactivation gate	0.33	462	0.074	NBD-Glu	membrane surface		521	0.113			33.3	15‡‡	13–25

\*Abbreviations used: ANT-TTX, anthraniloyl-C<sub>6</sub> tetrodotoxin; DACA-Lqq/Css, 7-dimethylaminocoumarin-4-acetamide—LqqV/Css; NBPM-SH-Lqq, *N*-[P-(2-benzoxazolyl)-phenyl]-succinimoyl-thioamidyl-Lqq V; NMAG-TTX, *N*-methylantraniloylglycine-C<sub>6</sub>-tetrodotoxin; BTX-NMA, batrachotoxinin-A-20  $\alpha$ -*N*-methylantranilate; NBD-Lqq, 3-(7-nitrobenz-2-oxa-1,3-diazol-4-yl) methylamino-acetamide-Lqq; NBD-glucosyl-*N*-methylphosphatidylglycerol

‡ $\phi$  is the quantum yield,  $\lambda_{em}^{max}$  is the wavelength of the fluorescence emission maximum in nm, and  $r_b$  is the fluorescence anisotropy of the bound probe.

§Efficiency per acceptor measured by quenching of the donor fluorescence

||Efficiency per acceptor measured by the sensitized emission of the acceptor

¶Distance assuming  $K^2 = 2/3$  Å

\*\*In the presence of 1  $\mu$ M Lqq V

‡‡Distance of closest approach (L)

extend over large distances from the Lqq binding locus. The fluorescence properties of DACA-Css bound to the channel are blue-shifted 10 nm in the presence of Lqq V. Taken with the distance measurement of TTX to Lqq and Lqq to Css and the conformational transition associated with the distance upon ligand binding, this information suggests a conformationally flexible channel with coupling of sites through the polyatomic framework of individual subunits or through alterations in subunit/subunit interactions.

We have developed a working model (Fig. 1) for the three-dimensional structure of the voltage-dependent sodium channel from the fluorescence spectral data, resonance energy transfer measurements between receptor sites on the channel and lipid headgroups at the membrane surface, and available biochemical data (6–8). The TTX/STX binding site is placed in a highly polar environment at the extracellular face of 270,000-dalton tubular trans-membrane structure of dimensions 40  $\times$  170 Å that has been solubilized and reconstituted and represents the ion conduction pore of the channel (6, 7). The TTX/STX-binding component is composed of three units of molecular weight 250,000 ( $\alpha$ ), 39,000 ( $\beta$ 1), and 37,000 ( $\beta$ 2), where

the  $\beta$  is associated with the unit through disulfide bonds. Affinity labeling with photoreactive Lqq-(8) and Css-derivatives (8a) specifically label the same peptide components of the channel. Radiation inactivation of the STX, Lqq, and Css receptors indicate target sizes of 256,000 mol wt for TTX and Lqq, and 41,000 mol wt for Css (Angelides, K. J., T. J. Nutter, L. N. Elmer, and E. S. Kemper, unpublished experiments). Equilibrium binding measurements on synaptosomes suggest that the ratio of TTX:Lqq receptors is  $\sim$ 3:1 (9), while the TTX:Css and BTX:Lqq ratios are 1:1 (9). From the experimentally determined depth of 15 Å of the Lqq binding site, the distances between this site and the BTX and Css, and the externally placed TTX sites, triangulation yields the inter-TTX distances shown in Fig. 1. The suggestion of a trimeric complex has been explored by energy-transfer measurement in which a low donor-TTX concentration was randomly mixed with varying acceptor-TTX concentrations. Quenching of donor fluorescence by increasing mole fractions of acceptor gives the distance of closest approach of the TTX to TTX sites of 50–70 Å. When 1.50 Triton X-100, known to solubilize the TTX receptor, is added, relief of quenching is observed, indicating a disruption of

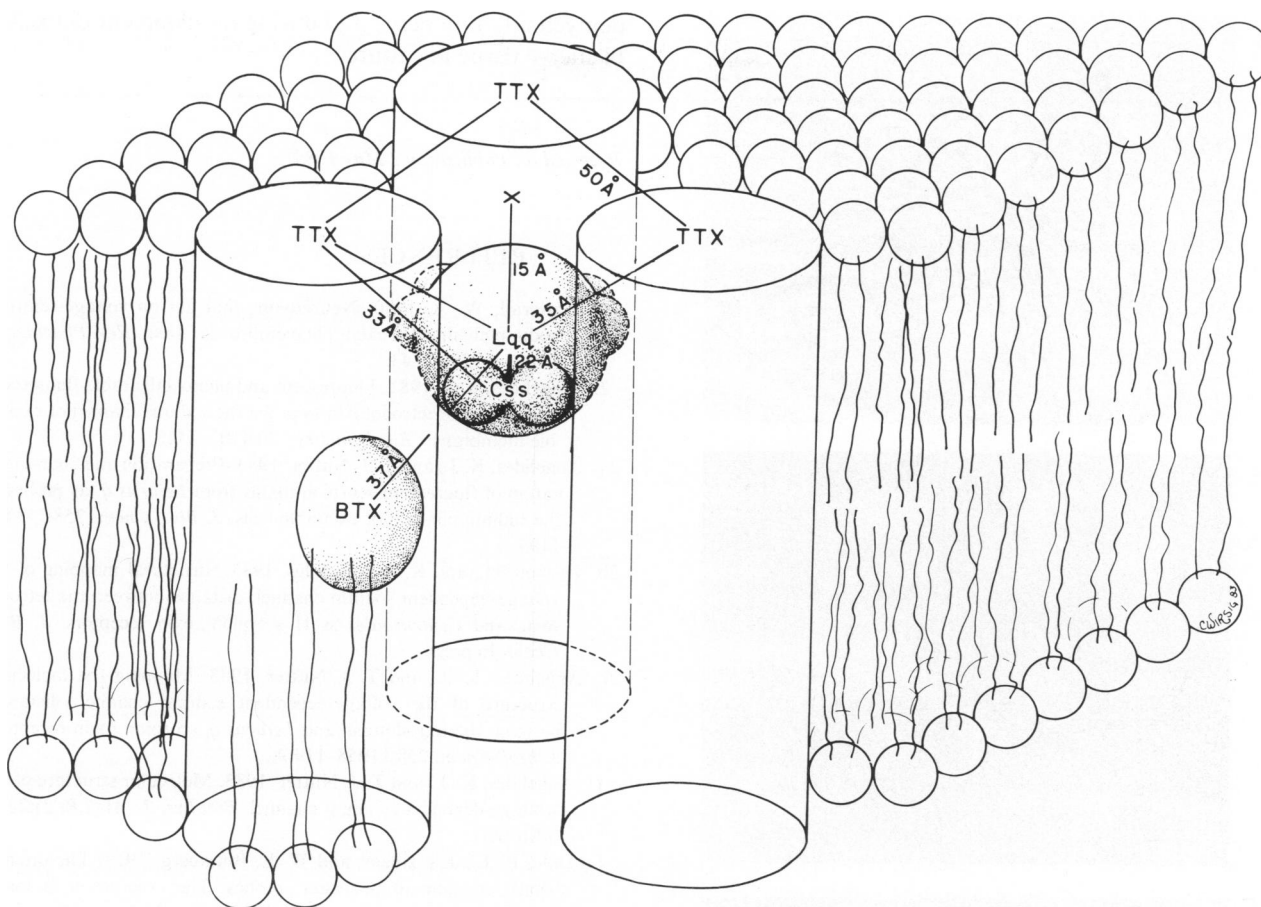


FIGURE 1 Representation of the three-dimensional molecular topology of the voltage-dependent sodium channel determined by resonance energy transfer between receptor sites and the membrane surface, in conjunction with available biochemical data.

the interaction between TTX sites. We are unable to determine whether there are two or more interacting or closely spaced TTX units, but the resonance energy-transfer measurements clearly indicate that at least two TTX receptors are closely arranged. We have therefore represented the molecular structure channel with three TTX binding components forming the ion-conducting pore of the channel centered on a 39,000 mol wt regulatory gating subunit ( $\beta 1$ ) for activation and inactivation that includes both the  $\alpha$  and  $\beta$  scorpion toxin receptors. The size of the BTX receptor is not known but is represented here in a hydrophobic environment directly interacting with the hydrophobic interior of the lipid bilayer and the  $\alpha$  subunit. The Lqq receptor is coupled to the BTX receptor through an association and coupling with the ion pore. We view the allosteric interactions between the BTX and Lqq sites as an alteration of the conformation of the TTX ion conducting pore that then transmits these changes as a distance change in the  $\beta 1$  subunit.

#### Cellular Mapping of the $\text{Na}^+$ Channel

The variety of our channel-specific fluorescent neurotoxins allows us to localize  $\text{Na}^+$  channels in nerve and muscle

fibers microscopically, and to determine  $\text{Na}^+$  channel distribution in these excitable tissues in normal and pathological states. NBD-Lqq V and DNP-Lqq V in particular have been extremely useful. NBD-Lqq has a very low fluorescence ( $\Phi = 0.012$ ) in solution but is substantially enhanced when bound to the channel ( $\Phi = 0.4$ ). The fluorescence emission of this labeled toxin is well-suited to fluorescence microscopy because of the high quantum yield and because conventional fluorescein emission filters can be used. Further, in situations where the channel density is low, the fluorescence signal may be amplified by applying an immunocytochemical technique with rabbit anti-DNP IgG (the NBD chromophore is a structural and functional analogue of DNP) followed by FITC-Protein A. The TRITC-Protein A may also be applied as a colloidal gold suspension so that subsequent to fluorescence microscopy, quantitative ultrastructural studies using electron microscopy can be performed. Fig. 2 shows a video-enhanced photograph of a single fiber from mouse sciatic nerve specifically stained for sodium channels utilizing the immunocytochemical approach described above. Experiments are currently in progress to determine the distribution and lateral diffusion of channels following acute

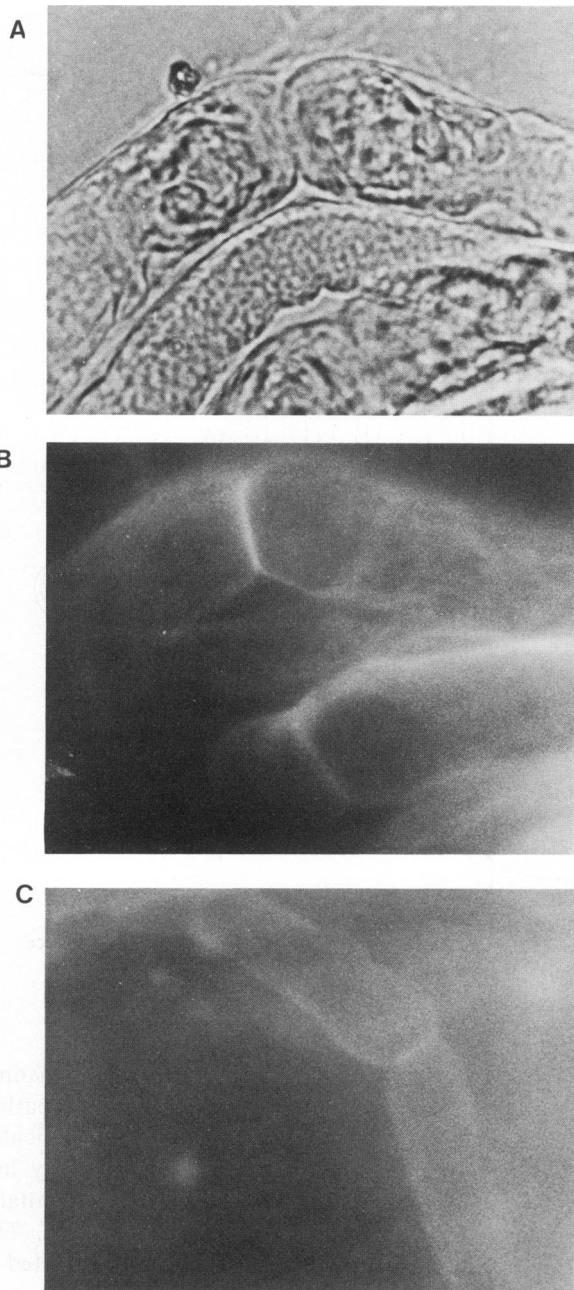


FIGURE 2 Video-enhanced fluorescence micrograph of a single myelinated fiber from mouse sciatic nerve stained for sodium channels with DNP-Lqg, and rabbit anti-DNP IgG/TRITC-Protein A (B). A, phase-contrast micrograph of the same field; C, identical conditions as B, but in the presence 1  $\mu$ M unlabeled Lqg.

demyelination in nerve and during development of excitable nerve tissue in culture.

Received for publication 2 May 1983.

## REFERENCES

1. Catterall, W. A. 1980. Neurotoxins that act on voltage-sensitive sodium channels in excitable membranes. *Annu. Rev. Pharmacol. Toxicol.* 20:15-43.
2. Angelides, K. J. 1981. Fluorescent and photoactivatable fluorescent derivatives of tetrodotoxin to probe the sodium channel of excitable membranes. *Biochemistry.* 20:4107-4118.
- 2a. Angelides, K. J., and T. J. Nutter. 1983. Preparation and characterization of fluorescent scorpion toxins from *Leiurus q.* as probes of the sodium channel of excitable cells. *J. Biol. Chem.* 258:11948-1195.
- 2b. Darbon, H., and K. J. Angelides. 1983. Structural mapping of the voltage-dependent sodium channel: distance between the tetrodotoxin and *Centruroides* ss II scorpion toxin receptors. *J. Biol. Chem.* In press.
- 2c. Angelides, K. J., and T. J. Nutter. 1983. Mapping the molecular structure of the voltage-dependent sodium channel: distances between the tetrodotoxin and *Leiurus q.* scorpion toxin receptors. *J. Biol. Chem.* 258:11958-11968.
3. Angelides, K. J., and T. J. Nutter. 1983. Molecular structure of the voltage-dependent sodium channel. *Biophys. J.* 41(2,Pt.2):224a. (Abstr.)
4. Dale, R. E., J. Eisinger, and W. E. Blumberg. 1979. The orientational freedom of molecular probes. The orientation factor in intramolecular energy transfer. *Biophys. J.* 26:161-194.
5. Dewey, T. G., and G. G. Hammes. 1980. Calculation of fluorescence resonance energy transfer on surfaces. *Biophys. J.* 32:1023-1036.
6. Hartshorne, R. P., and W. A. Catterall. 1980. Purification of the Saxitoxin receptor of the sodium channel from rat brain. *Proc. Natl. Acad. Sci. USA.* 78:4620-4624.
7. Ellisman, M. H., W. S. Agnew, J. A. Miller, and S. R. Levinson. 1982. Electron microscopic visualization of the tetrodotoxin-binding protein from *Electrophorus electricus*. *Proc. Natl. Acad. Sci. USA.* 79:4461-4465.
8. Hartshorne, R. P., D. J. Messner, J. C. Coppersmith, and W. A. Catterall. 1982. The saxitoxin receptor of the sodium channel from rat brain. *J. Biol. Chem.* 257:13888-13891.
- 8a. Darbon, H., E. Jover, F. Coaraud, and H. Rochat. Photoaffinity labeling of  $\alpha$ - and  $\beta$ -scorpion toxin receptors associated with rat brain sodium channels. *Biochem. Biophys. Res. Commun.* 115:415-422.
9. Catterall, W. A., C. S. Morrow, and R. P. Hartshorne. 1979. Neurotoxin binding to receptor sites associated with voltage-sensitive channels in intact, lysed, and detergent-solubilized brain membranes. *J. Biol. Chem.* 254:11379-11387.